Near-wall flow features in ZPG-TBL at various Reynolds numbers using dense 3D Lagrangian Particle Tracking

Andreas Schröder*[1,2], Daniel Schanz[1], Reinhard Geisler[1],
Philipp Godbersen[1], Janos Agocs[1] and Abhijna R. Simhan[2]

1. German Aerospace Center (DLR), Inst. of Aerodynamics and Flow Technology, Göttingen, Germany
2. Institute of Transport Technology, Brandenburg University of Technology, Cottbus, Germany
* Corresponding author: Andreas.Schroeder@dlr.de

Keywords: Coherent structures, wall-bounded flows, turbulence, Shake-The-Box, FlowFit

Abstract

The 3D Lagrangian particle tracking method *Shake-The-Box* (STB) [1] and, subsequently, the data assimilation method *FlowFit3* [2][3] have been applied to measure the flow field in a narrow wall-parallel volume inside the near-wall region of a zero-pressure-gradient (ZPG) turbulent boundary layer (TBL) flow at various Reynolds numbers. The STB experiments have been conducted in the 1m- wind tunnel facility of DLR in Göttingen at relatively high particle image densities (~0.07 ppp) using µm-sized DEHS particles and high-repetition pulse laser at up to 38.1 kHz. The results show that the chosen methodology is able to volumetrically resolve almost all features of the flow inside the viscous sub-, buffer- and lower logarithmic- layer in space and time at Reynolds numbers up to Re_θ = 5,455. The gained data consists of time-series of spatially well resolved 3D velocity, acceleration and pressure fields, as well as a huge amount of long Lagrangian particle trajectories. Selecting the viscous sublayer part of the measurement volume provides time-series of the 2D distributions of both components of the instantaneous wall-shear stresses $\tau_{w,x/z}$. The resulting data are used for conditional and time-resolved 3D analyses of coherent structures, like sweep-streak interactions, rare (e.g. back flow) events and two-point space-time-correlations.

1. Introduction

ZPG-TBL flows at technically relevant Reynolds numbers continue to attract a great deal of attention in fluid mechanics. The reason for this is the wide range of spatial and temporal scales that play a role in the transport of turbulent kinetic energy from the outer flow to the wall and its backscattering, involving the so-called "near-wall cycle". Especially, the role of coherent flow structures of various wave-numbers during the interaction of the flow with the wall is not fully understood. For example, local back-flow events close to the wall and thus negative wall-shear stress are rare phenomena in ZPG-TBL and locally often caused by spanwise inclined vorticity [4][5]. However, so far only few experimental data are available [6][7], which up to now cannot support statistically evident insights into the involved 3D flow structure dynamics and topologies, which could allow to unfold a cause-and-effect chain of their spatial and temporal development. On the other side, high wall-shear stress (τ_w) events contribute significantly to viscous drag of moving vehicles due to related strong wall-normal velocity gradients close to the surface. Thus, it is of great importance to enhance the understanding of the dynamics of extreme τ_w events, related sweep- (Q4) -streak interactions and ejections (Q2), both from a fundamental and an engineering point of view.
However, most of the known measurement techniques are confronted with significant challenges in providing reliable experimental data in close proximity to the wall at relevant Reynolds numbers mainly due to the presence of large mean and instantaneous velocity gradients. The use of accurate and miniaturized probe measurement techniques is still limited in such flows due to its intrusiveness (e.g. stagnation points and induced pressure gradients), susceptibility for vibrations, coupling effects with the wall and its spatial extensions, which might cause low-pass filtering effects of the instantaneous velocity or pressure measurements. In contrast, a 3D LPT approach can be specifically favorable, because small particles (e.g. at

~1.5 µm diameter) at Stokes numbers below St << 0.1 can be considered as fluid elements in the investigated incompressible TBL flow. Therefore, in this work, we propose using dense 3D Lagrangian particle tracking by STB over long time series to volumetrically achieve all relevant turbulent flow measures in the near-wall region. It is common knowledge that for all wall-bounded flows the mean skinfriction velocity u_τ is of eminent importance for scaling the boundary layer flow connected with attached eddies by viscous units, which allow collapsing the mean velocity and Reynolds stress profiles normal to the wall up to the outer logarithmic region of a TBL flow. Nevertheless, actually wall-shear stresses in both wall-parallel directions are fluctuating signals including strong intermittent events. Therefore, the dynamics of near-wall flow structure mechanisms in relation to the fluctuation of wall-shear stresses still need to be further analyzed. The existing large data-set at four Reynolds numbers can support addressing such questions with sufficient statistical evidence. In order to obtain the desired instantaneous friction velocity distribution u_τ and wall-shear-stress τ_w components and its mean and fluctuation values a local gradient estimation has to be calculated from the measured individual particle tracks in close proximity of the wall ($y^+ < 4.5$).

$$u_\tau = \sqrt{\frac{\tau_w}{\rho}} = \sqrt{\nu \frac{\partial u}{\partial y}|_{y=0}} \quad \text{with} \quad \tau_{w,x} = \mu \frac{\partial u}{\partial y}|_{y=0}.$$

The spanwise wall-shear stress component $\tau_{w,z}$ can be obtained in an analogue way by the wall-normal gradient of the w-component of the instantaneous velocity vector. Nevertheless, the rms-value of the spanwise wall-shear stress component is slightly decreasing over the viscous sublayer with wall-distance so that the width of the corresponding PDF would be slightly underestimated if the measurement for the differential quotient $\mu\Delta w/\Delta y$ is calculated with values e.g. y+ > 2 in order the allow for a higher accuracy due to the uncertainties of the involved measures, specifically of the particle's wall distance in the denominator, which in an ideal case should be as small as possible. The accuracy of the required wall-normal gradient estimation is limited by the position uncertainty of the particle track and the one of the wall, as well as by the uncertainty of the particle's velocity vector measurement. Therefore, a decent uncertainty quantification is necessary for the statistics of the wall-shear stresses with respect to the wall distance. Such an uncertainty quantification is available a-posteriori on the basis of the TrackFit [2] approach used for the optimal temporal filtering. With the present Lagrangian particle tracking data located inside the viscous sublayer both components of the instantaneous wall-shear stresses are available at relatively high spatial resolution and accuracy for the range of the investigated Reynolds numbers (see Table 1). In the following we will explain how to gain optimized results for all three measures required to obtain wall-shear stresses, for time-resolved velocity and pressure fields in the whole measurement volume (up to the lower logarithmic layer) and for providing statistical convergence for the related PDFs, single- and two-point statistics using 3D LPT measurements by STB and FlowFit3 data assimilation.

2. Experimental set-up and procedure

The measurement campaign was performed in the closed test section of the 1m-wind tunnel at DLR Göttingen with a cross-section of 740 x 1,000 mm^2 and a test section length of 3,000 mm. At four free stream velocities of U_∞ = [7.5; 10; 15, 20] m/s a boundary layer flow develops along x = 2.08 m at the lower wall of the test section with 1 m spanwise extension to a ZPG-TBL flow at Reynolds numbers based on the momentum thickness in the range between Re_θ = [2,306; 5,455] (values from previous measurements [8], see Table 1). The boundary layer was tripped by zig-zag bands right after the contraction section and its thickness at the measurement volume is slightly decreasing with the Reynolds number in the range of δ_{99} = [38.12; 34.37] mm. DEHS particles with a mean diameter of ~1.5 µm were generated by a Laskin nozzles type seeder and homogenously distributed inside the circuit wind tunnel. The particles within the measurement volume of ~60 x 15 x 2 mm³ were illuminated by a *Photonics Ind. DM200* laser from the downstream end of the test section. The illuminated particles were imaged on a system of five high-speed cameras (4 x Phantom v2640 + 1 x v1840, see Figure 1) equipped with Scheimpflug mounts and with sensors cropped in spanwise direction to allow for the high repetition rates required (up to 38.1 kHz). In order to avoid pixel-locking of the particle image

position measurements with the given camera pixel size of 13.5 µm in both directions of the CMOS sensors the f = 100 mm *Zeiss macro planar* lenses focus were placed parallel to the wall and slightly above the measurement volume of y= 2 mm height in depths direction of the cameras. In this way particle image diameters between maximal 4 pixels very close to the wall surface and 2 pixels at the upper plane of the illuminated volume could be achieved at an aperture of $f_\# = 4$. The cameras were calibrated using a 3D calibration plate *Type 11* from *LaVision* with subsequent refinement using Volume-Self-Calibration [9] and a calibration of the particles Optical Transfer Function [10].

Table 1 ZPG-TBL flow test matrix

U_∞[m/s]	Re_τ	Re_Θ	Viscous unit µm	Acquisition freq [kHz]	Sensor size	Images per run	Number of runs
7.5	793	2306	48.1	18.0	2048 × 512	85,000	10
10	995	2997	37.0	23.9	2048 × 512	85,000	10
15	1352	4160	25.5	30.0	2048 × 400	115,000	12
20	1762	5455	19.5	38.1	2048 × 304	140,000	10

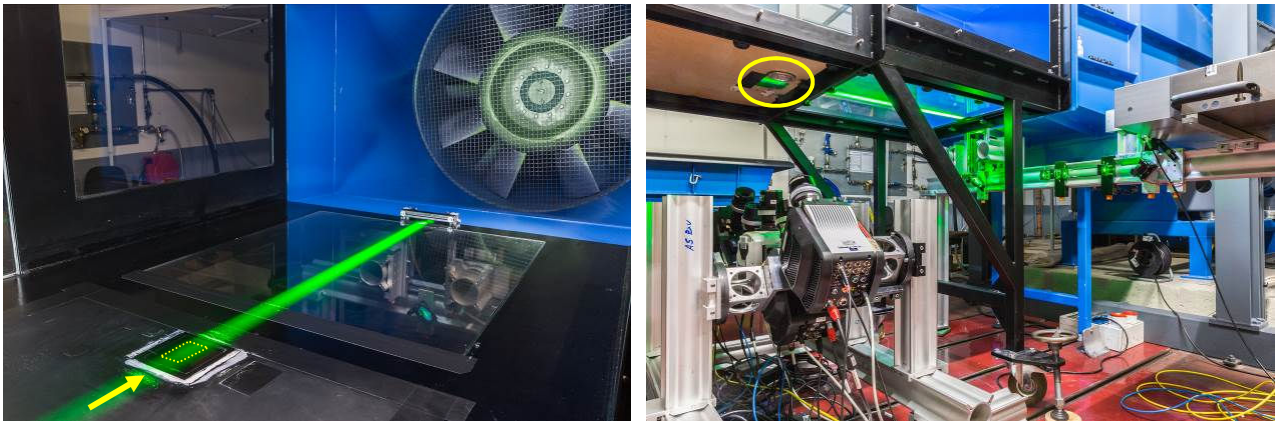

Figure 1 *Experimental set-up at the 1m-Wind Tunnel of DLR Göttingen. Left: Illuminated laser light volume by 2 x Photonics Ind. DM200 close to wall with indication of flow direction and imaged area. Right: Five high-speed cameras (4 x Phantom v2640 + 1 x v1840) viewing in an in-line setup at 90° particle light scattering into a measurement volume of ~60 x 2 x 15 mm³ (in flow-, wall-normal and spanwise- directions) from below the test section.*

Images were captured with a particle image density of around ~0.06- 0.07 particles-per-pixel (ppp). Depending on the image resolution (see Table 1) up to ~70,000 particles have been tracked simultaneously over several long time series of up to 140,000 consecutive images by STB [1]. The resulting velocity and acceleration values have been used as input for *FlowFit* [2][3], which delivers highly resolved 3D velocity and pressure fields using Navier-Stokes- constraints.

3. Wall-position and -vibration corrections

An exact positioning of the wind tunnel wall for every recorded time-step is necessary for the generation of high-resolution profiles and specifically the estimation of the instantaneous wall-shear-stresses. Effects of vibrations (for the wind tunnel wall as well as for the inter-camera alignment and the time-depended shifts of the LOS relative to the wall), tilt of the calibrated volume in regards to the real wall and a general shift have to be accounted for. The glass window, through which the five cameras were observing the flow, was regularly cleaned and does not provide information about the wall position (e.g. by sticky particles or other light scattering artefacts). Therefore, a method was developed to correct for vibration and tilt with respect to the initial calibrated coordinate system directly from the tracked particles.
Here a new methodology for vibration corrections of 3D STB measurements in close proximity to the wall is proposed which does not rely on wall markers e.g. given by sticky particles or dust etc. These wall particles

do have unfavourable light scattering properties and do not behave like a point source because of their typical non-spherical shape. This does not allow to detect the centre of it in all three dimensions at high accuracies from its diffraction limited particle image. Therefore, we introduce a method based on the µm sized spherical tracer particles itself: After tracking by STB a selection of low velocity particles was made, specifically particles with streamwise velocities less than u = 0.2 m/s and wall-normal velocity magnitudes less than v = 0.03 m/s were chosen. Furthermore, slow-moving particles affected by flow behaviour outside the lower viscous sub-layer were excluded by limiting the height of the selected sub-volume using an initial approximation of the wall-position. In such a selection, particles can be considered to be almost "glued" to the wall with respect to their y-position over short time sequences as they are mostly located at $y+ < 0.5$ in the very lower part of the viscous sublayer. These particles are indicating both: a) the true planar wall-orientation by averaging them in a 3D distribution over the whole time-series for tilt correction of the calibrated camera system and b) the wall-normal oscillations from the structural vibrations by averaging them over the whole domain and additionally for relatively short moving-average time windows to achieve a 1D signal in y-direction for vibration corrections.
The apparent tilt in the measurement volume with respect to the orientation of the calibration target, which defined the original coordinate system, was estimated using a plane of best fit along these selected 3D particle data which was used for rotational correction of the wall-normal vector (see Fig. 2 (left)).
Followed by this, the same slow-moving particles were averaged with a moving window over 50 time-steps each (temporal oversampling of the structural vibration frequency is provided by a factor >500) to obtain accurately the mean wall-normal distance along the vibration oscillations (see red curve in Fig. 2 (right)). This accurately measured the single-time-step vibration amplitude, for which the prior mode of oscillation was found to be in the range around 30 Hz, in a well sampled fashion as our image acquisition frequency was 30 kHz for the presented U_∞ = 15 m/s case and temporal filtering of the tracks enhanced the particle's position accuracy by a factor 2. As the position uncertainty of the filtered particle tracks can be assumed to be Gaussian noise a large number of tracks and time steps used for this approach can massively reduce the error in determining the correct amplitudes by 1 over the square-root of used particle samples N_p. Furthermore, the vibration correction was implemented iteratively which brought down the amplitude of vibration from an initial rms-value of ~10 µm to less than 0.4 µm after only two iterations (see green line in Fig. 2 (right)), which in the second iteration as well allows to exclude further particles which might not be well "glued" to the wall and follow fluid dynamical dynamics not strongly correlated with the wall vibrations.

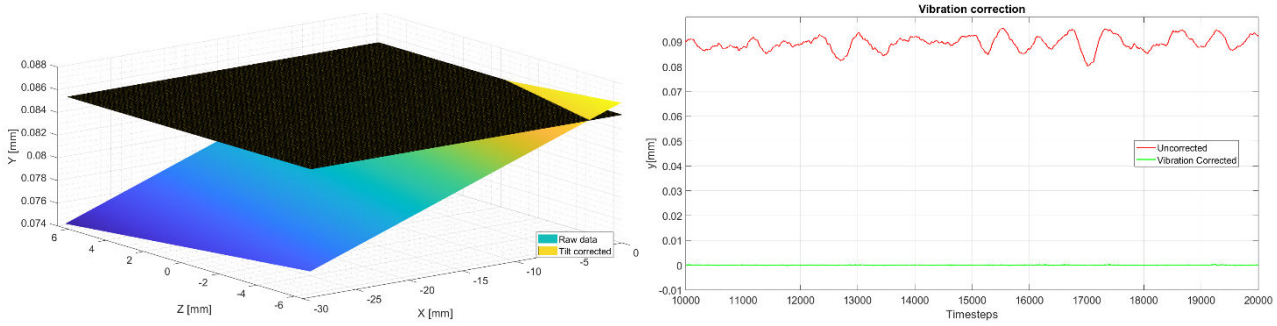

Figure 2 *Data fit of plane over 3D average of selected low velocity particles before and after tilt correction (color coded by wall-normal height) (left) and subsequent single time step off-set- and vibration correction by two iterations using the same selection of particles very close to the wall for a 1D moving time-window average (right)*

The exact final wall position [11] was then extracted from spatially highly resolved mean velocity profiles using bin averaging of the STB tracks in bin sizes of 1 µm or for this case 1/25th of a viscous unit at four sub-volume locations and extrapolating the linear profile between $2 < y^+ < 4.5$ to zero *u*-velocity. After estimation and final shift correction of the wall position by a few µm, span- and streamwise symmetry in a statistical sense for the relatively small volume can be assumed, so that wall normal 1D-profiles and two-point-correlations with a very high spatial resolution can be extracted and reliable data assimilation approaches can be applied with imposing no-slip boundary conditions at the wall.

4. Results and discussion

Fig. 3 (left) shows the four relevant Reynolds stresses (<u'u'>, <v'v'>, <w'w'> and <u'v'>) (not normalized by u_τ yet) with a zoom into the near-wall region $y^+ < 20$ for the U_∞ = 15 m/s or Re_θ.= 4,160 case. It is remarkable how smooth the Reynolds stresses converge to zero when approaching the wall in a component-wise expected manner. A direct comparison of the mean and Reynolds stress statistics with DNS data of TBL at very similar Reynolds numbers from Schlatter et al (2010) [12] over this y^+-range of the measurement volume shows excellent agreement. From the results of the full STB evaluation we achieved resolutions of statistically converged wall-normal profiles of velocity- and acceleration mean and variances down to bin sizes of ~2 µm using the full number of runs. In Fig. 3 (right) the PDFs of the u-velocity component collected in two 5 µm sized bins at y^+ = 1.5 and y^+ = 5 normalized by the respective rms-values are shown. Please be aware of the differences of the two rms-values (see variances of <u'u'> in Fig. 3, left) .The preliminary statistics are based on only two of 10 runs, but already ~1.5 million entries show rare intermittent backflow events for the bin in close proximity to wall and for both a skewness of the PDF maxima towards low u-velocities, while an extended branch of seldom high u-velocity events (indicating intermittent high wall-shear stress) can be seen again more prominent for the bin at y^+ = 1.5.

In order to present the quality and spatial resolution of the results Lagrangian particle tracks from STB and vortical flow structures by the Q-value iso-contour-surfaces, gained by the application of FlowFit to the tracking results, are shown for individual time-steps for the three higher Re-number cases within Figures 4 to 9. An example of ~60,000 measured instantaneous velocity and acceleration vectors at U_∞ = 10 m/s within the wall-parallel volume of approximately 60 x 2 x 15 mm³ according to 1620 x 54 x 405 viscous units $(l^+)^3$ in x-, y- and z-directions is shown in Fig. 4, left and right respectively. The velocity vectors are color coded by the u- and the acceleration vectors by the x-component both calculated from the first and second temporal derivative of a 3rd order B-Spline filter ('TrackFit') [2] applied to the 3D Lagrangian particle tracks. In Figure 5 typical features of a turbulent boundary layer flow in close proximity to the wall like low- and high-speed streaks and streamwise-, cane- and hairpin-like vortices can be identified from a data assimilation result gained by FlowFit3 [3]. In a full movie animation of the time-series events of sweep-streak interactions and the temporal development of ejections and new streamwise- and cane vortices can be investigated in detail. In Figure 6 a wall-parallel slice of the same instantaneous FlowFit3 vector field result extracted at y = 180 µm height corresponding to $y^+ \sim 4.8$ within the upper part of the viscous sub-layer with color coded u-velocity component is presented. The low-speed streaks are narrower in spanwise directions and more elongated in flow direction than the high-speed streaks, which is in accordance with the literature. Nevertheless, the chosen experimental approach demonstrates here a high spatial velocity field resolution for a single slice of the full FlowFit volume. Data assimilation of the LPT input data by FlowFit can provide highly resolved velocity, acceleration and pressure volumes in time steps of 41.84 µs over 10 time-series of in total 35.5 seconds for the U = 10 m/s case and according to Table1, as well for the other flow cases. A decent analysis of the spatial and temporal interaction of Lagrangian particle properties, the instantaneous flow topologies (e.g. vorticity/enstrophy and regions of high energy dissipation) and pressure fields will be wide field, which is beyond the scope of the present paper. Here, only a first presentation of relevant properties of the experimental STB and FlowFit data set in the four TBL flows shall be presented.

Fig. 7 shows particle tracks in a wall attached slice of 115 µm thickness or $y^+ < 4.5$ at Re_θ.= 4,160. The visible particle tracks (here given in streaks over 20 time-steps) directly represent the instantaneous flow structures in the viscous sublayer and thus the corresponding instantaneous wall-shear stresses [13][14] or friction velocities. As explained above a statistical characterization of the wall-shear stresses in flow- and spanwise directions is of high importance for scaling properties of TBL and for understanding (intermittent) flow separations scenarios e.g. in APG-TBL flows.

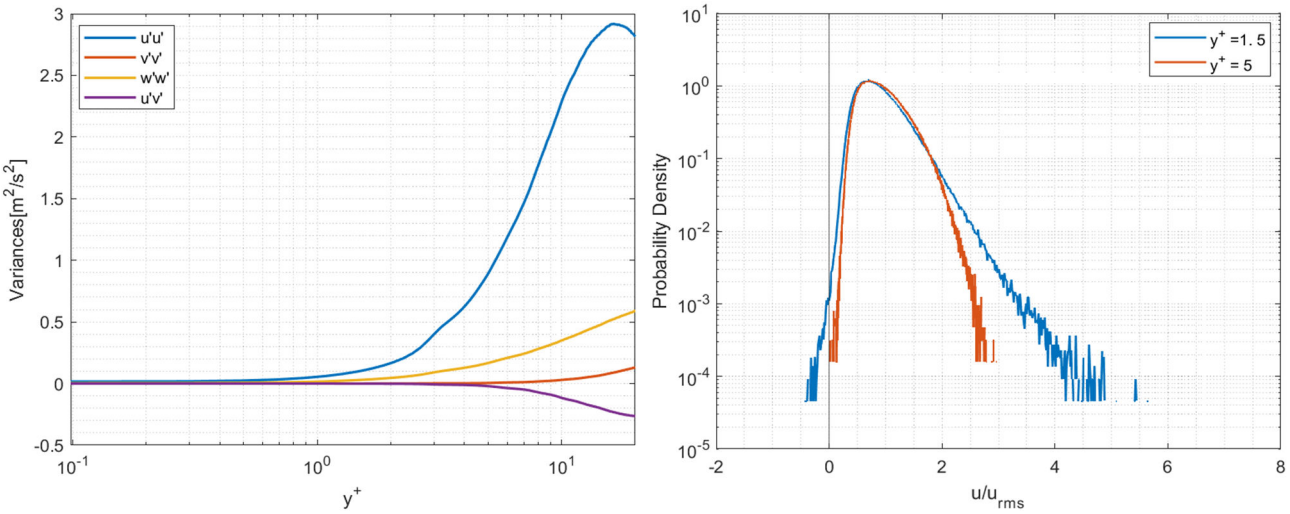

Figure 3 *Reynolds stresses in the near wall region $y^+ < 20$ based on bin-averages of 5 µm size in y-direction corresponding to ~1/5 th of l+(left) and PDF of the normalized u-velocity component for two bins at y^+ =1.5 and 5 (right) for U = 15 m/s or* Re_θ = 4,160.

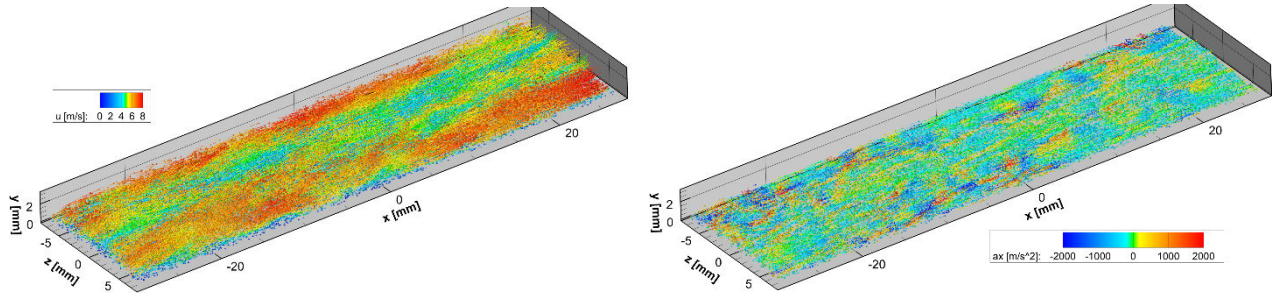

Figure 4 *Snapshot of particle tracks in the region between 0 < y+ < 54 color coded by u-velocity (left) and for a slice of 0 < y+ < 27 by the x-component of acceleration (right) for* U_∞ = 10 m/s at Re_θ = 2,990. *Tracking of approx. 60.000 particles per time-step. Position accuracy estimated from TrackFit: ~1.5 µm (~1/25 l+)*

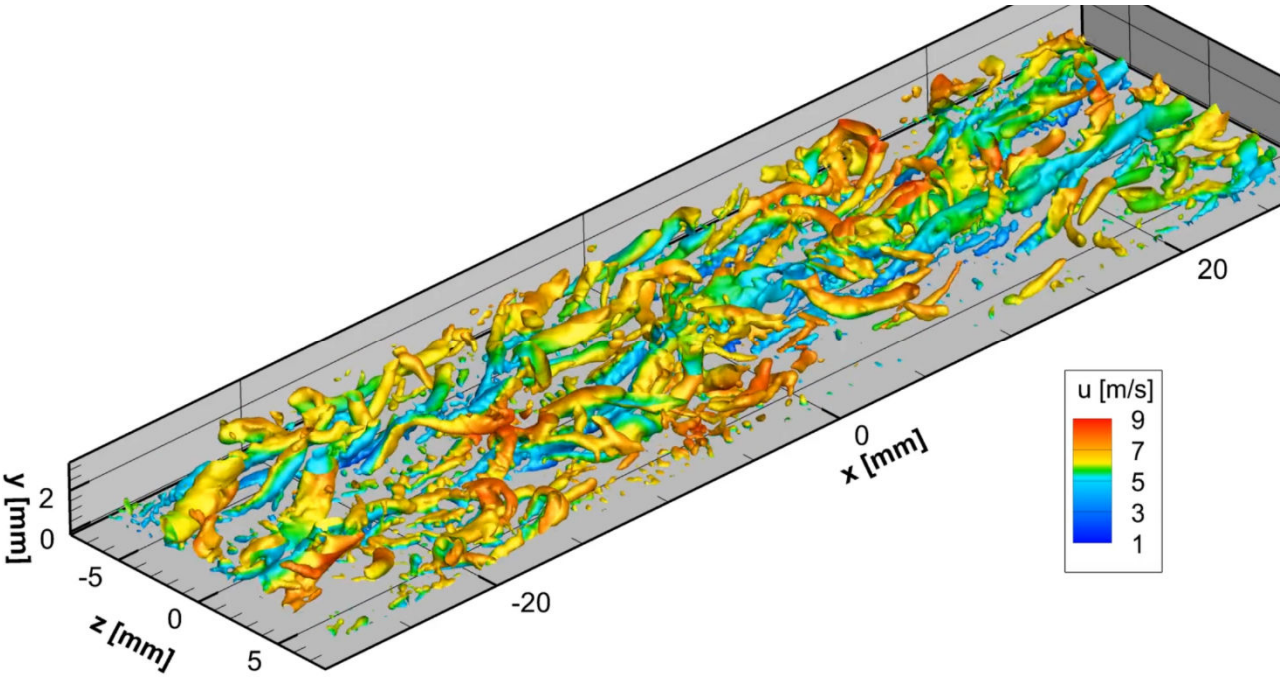

Figure 5 *Snapshot of time-resolved vortical flow structures in the region between 0 < y+ < 54 by iso-surfaces of Q-value (Q = 1,200,000/s²) color coded by u-velocity for* U_∞ = 10 m/s at Re_θ = 2,990

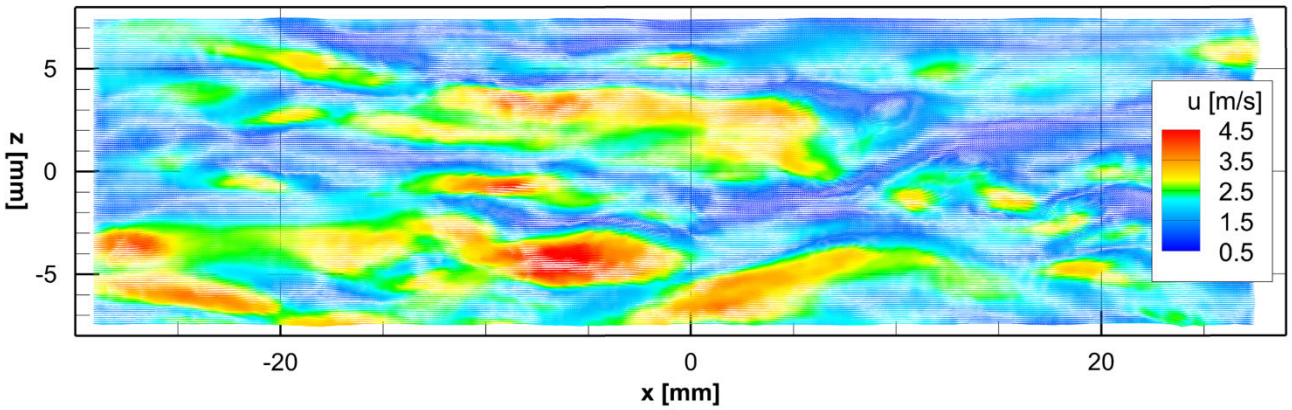

Figure 6 *Slice of the FlowFit data assimation of Fig. 5 at y ~ 180 µm corresponding to y+ ~ 4.8 showing near-wall streaky structures (narrower in spanwise directions for low speed streaks than for high speed ones)*

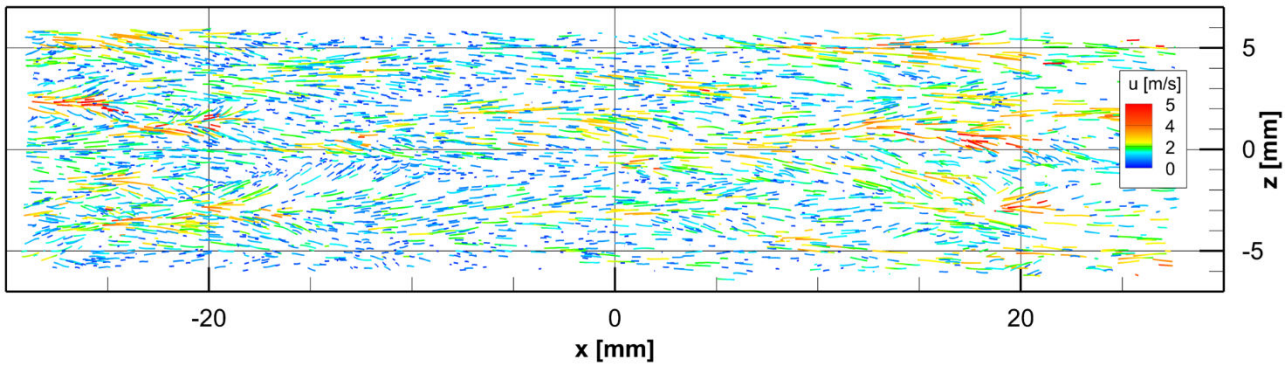

Figure 7 *Instantaneous particle tracks (20-time-steps) color coded by u-velocity in a 115 µm sliced volume between 0 < y+ < 4.5 for U_∞ = 15 m/s at Re_θ = 4,160.*

In Fig. 8 a snapshot result from a full time series visualizes flow structures in the region between 0 < y+ < 78 or 0 < y < 2 mm by iso-surfaces of Q-value at Re_θ.= 4,160. Here, at a higher Reynolds number the turbulent structures in the investigated region are becoming more fine-scale, but although the inner scaling viscous unit shrinks down to 25.5 µm still most of the (typical) vortical structures indicated by the Q-value iso-contour-surfaces and color coded by u-velocity are well resolved in space and in time. This time series will allow for investigating the dynamics of flow structures e.g. conditioned to certain flow events over a relatively large domain in flow direction.

In Figure 9 one can see a similar example of a FlowFit result for the TBL flow case at U_∞ = 20 m/s at Re_θ = 5,455. Due to the high imaging frame rate of 38.1 kHz the spanwise resolution was limited to 304 px, so that the spanwise extension of the volume is now limited to ~9 mm. On the other hand, with small viscous units of 19.5 µm the wall-normal extension of the measurement volume reaches now y^+ = 102. However, still the majority of vortical flow structures seem to be well resolved with only some visible under-sampling in close proximity to the wall. Please note that for all cases the time-resolved instantaneous 3D pressure distribution can be made available as well.

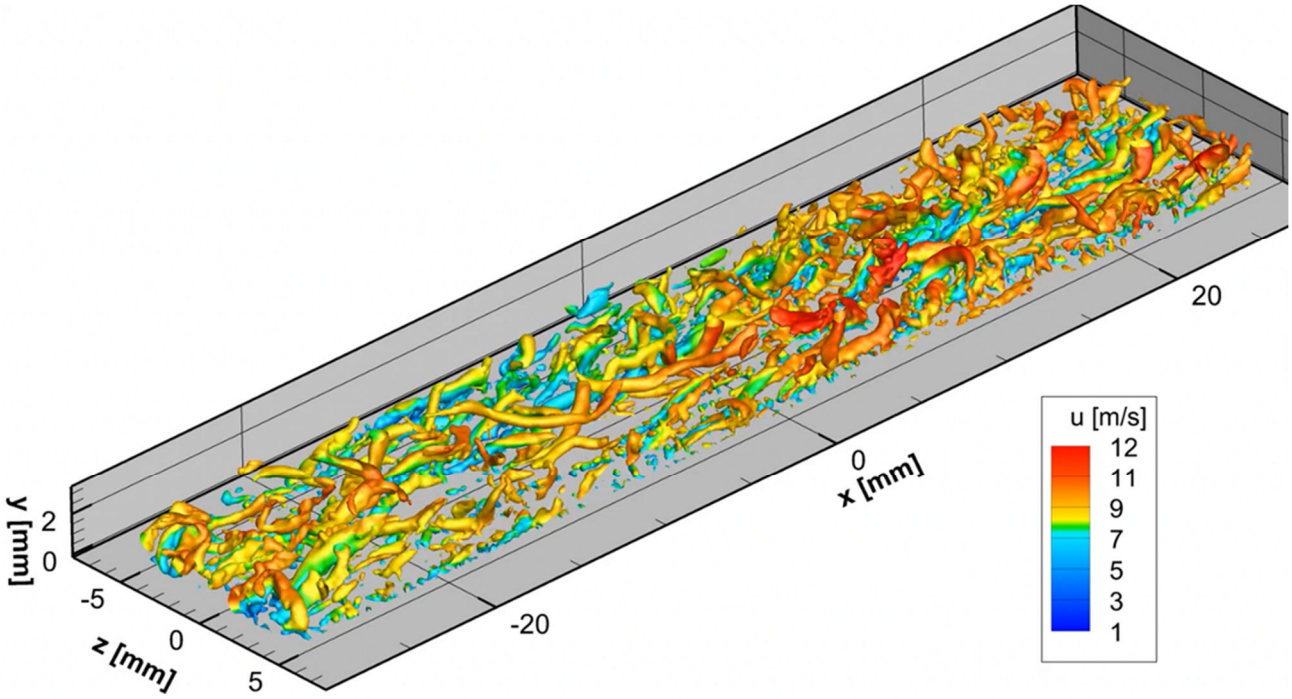

Figure 8 *Snapshot of time-resolved vortical flow structures in the region between 0 < y+ < 78 by iso-surfaces of Q-value (Q = 5,000,000/s²) color coded by u-velocity for U_∞ = 15 m/s at Re_θ = 4,160.*

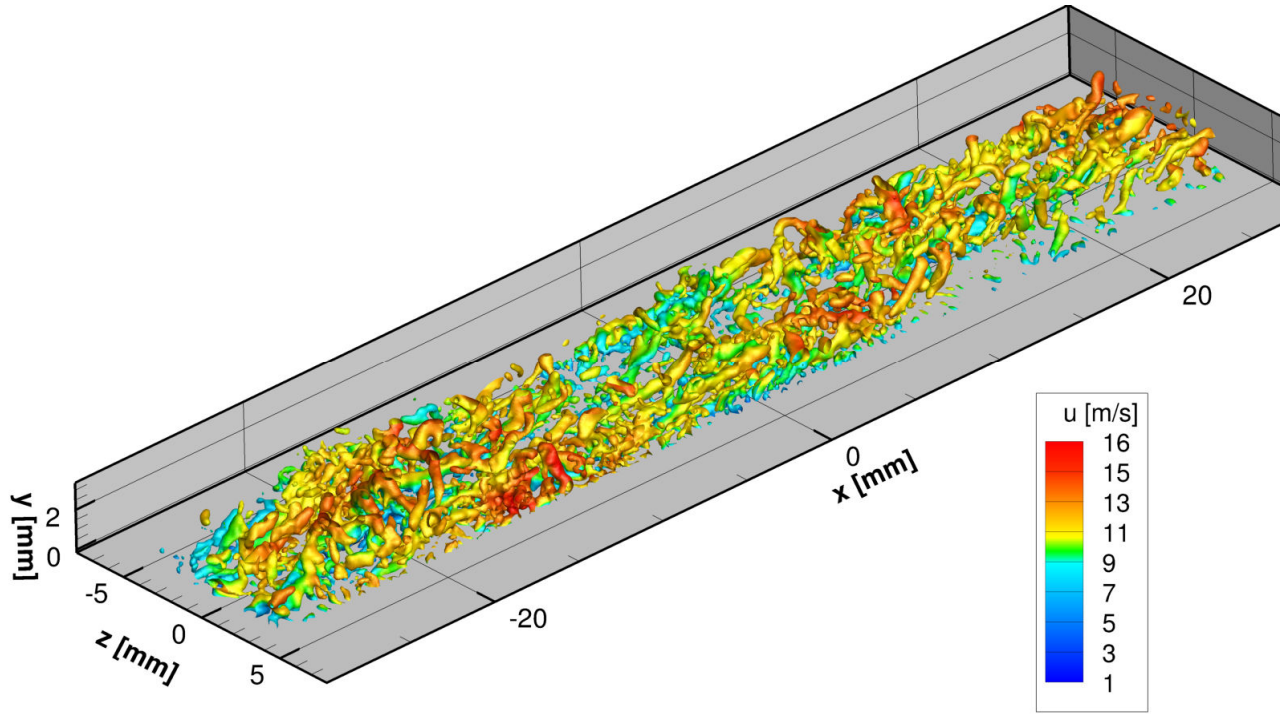

Figure 9 *Snapshot of time-resolved vortical flow structures in the region between 0 < y+ < 102 by iso-surfaces of Q-value (Q = 8,000,000/s²) color coded by u-velocity for U_∞ = 20 m/s at Re_θ = 5,455*

5. 3D two-point-correlation functions and joint PDFs of wall-shear-stress

A way to allow for a more general analysis of the extension and shape of coherent structures in the near-wall region is the calculation of 3D-two-point-correlation functions for the three velocity fluctuation components u', v'and w' or $u'_{i,j}$ (Eqn 1), which also provide statistical information of the involved Taylor micro- and macro scales and, in case of space-time-correlations, as well the related mean convection velocities and temporal decay of

the coherence of flow structures. The latter one would give as well an indication of the (local) validity of Taylor's frozen turbulence hypothesis.

$$R_{ij}(\Delta x,\Delta y,\Delta z,\Delta t)=\frac{\sum_x\sum_y\sum_z\sum_t\ u_i'(x,y,z,t)\ \cdot\ u_j'(x+\Delta x,y+\Delta y,z+\Delta z,t+\Delta t)}{\sqrt{\sum_x\sum_y\sum_z\sum_t\ u_i'^2\ (x,y,z,t)}\cdot\sqrt{\sum_x\sum_y\sum_z\sum_t\ u_j'^2\ (x+\Delta x,y+\Delta y,z+\Delta z,t+\Delta t)}}\qquad Eqn\ 1$$

Because of the high number of possible correlation functions of all velocity and acceleration components and other scalars, like vorticity and pressure from FlowFit, in time and space, which we shall be addressed in later publications, we restrict ourselves here to the description of the velocity and acceleration 3D two-point-correlations of the trace of the respective two-point correlation tensors. For the components of acceleration, the Eqn 1 can be used analogously with a_i and a_j as input values. In Figure 10 a representation of the two-point-correlation functions of $R_{u'u}$ (left), $R_{v'v'}$ (middle) and $R_{w'w'}$ (right) is calculated for a reference slice searching component-wise for particle velocity entries between 100 µm (y+= 3.9) and 150 µm (y+ = 5.9), which is centered approximately at y+ = 5 for Re_θ = *4,160*. These scalars are cross-correlated over the whole 3D measurement area by collecting and summing-up multiplied and rms-normalized values for all components of the two-point-correlation tensor in 300 µm sized bins in x- and z-directions and 50 µm slices in y-directions at the inter-particle distances dx, dy and dz. The same script calculated for the acceleration components for a reference area at y+ = 5 as shown in Figure 11. For the three shown correlations of the velocity components in Figure 10 the typical stream-wise elongated and streaky coherence can be observed for all three functions. At this wall distance the u'u' correlation functions (Figure 10, left) are elongated most in flow directions, which corresponds to the well-known near-wall streaks with spanwise alternating negative- and positive u' with an average distance of z+ ~ 100. This value can be estimated by the blueish spanwise separated areas along dx = 0 mm. Looking at the streamwise elongated v'v' correlation function (Figure 10, middle) one can see two distinct negative correlation areas with correlation values < -0.1. The spanwise distance of these two minima of ~z+ = 60 or ~1.5 mm indicate that the average distance of the maximal v' amplitudes of negative and positive values related to streamwise vorticity in that region is a bit smaller than the streaky pattern related to u'-velocities. For the w'w' correlation function (Figure 10, right) as well an elongation in stream direction is noticeable while a wider spanwise distribution of the positive correlation area here indicate that the next streamwise aligned vortex with a spanwise velocity component of opposite sign is in average located at a spanwise distance of ~ z+ = 150 or 3.8-mm. The responsible dynamic interplay of the involved instantaneous flow structures is washed out and symmetrized in the present two-point-correlation functions. Conditional, two-point-correlations based on positive and negative signs or selected by fluctuation amplitudes (e.g. > sigma) etc. can be calculated as well to establish a more general view on coherent structures.

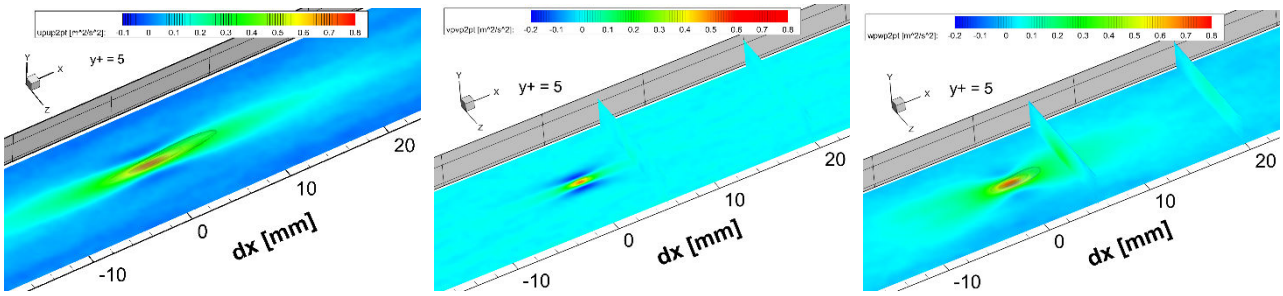

Figure 10 *3D two-point-correlation functions of the velocity fluctuation components $R_{u'u'}$, $R_{v'v'}$ and $R_{w'w'}$ at y+ = 5 or 125 µm wall-distance for the U = 15 m/s case at Re_τ = 1352 (bin averaging, arbitrary values)*

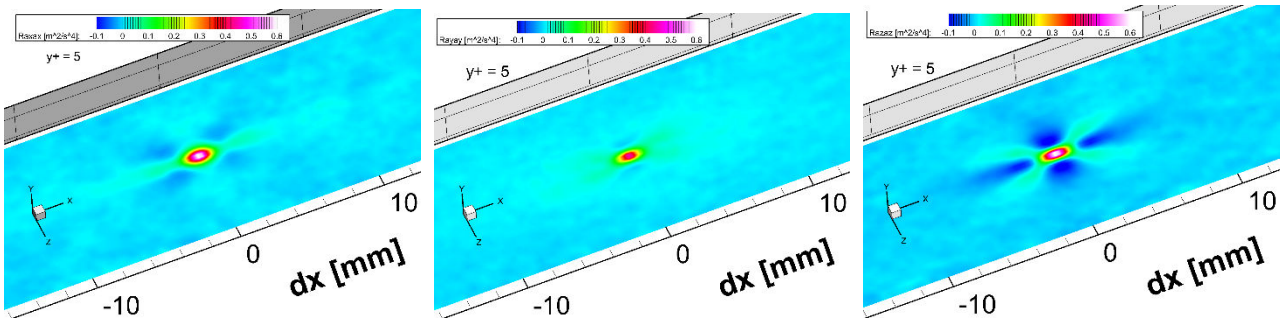

Figure 11 *3D two-point-correlation functions of the acceleration components R_{axax}, R_{ayay} und R_{azaz} at y+ = 5 or 125 µm wall-distance for the U = 15 m/s case at Re_τ = 1352 (bin averaging, arbitrary values)*

In Figure 11 for the first time, to the authors knowledge, 3D two-point space correlations of the individual components of the Lagrangian accelerations are displayed for a wall distance of y+ = 5. The shown patterns of the correlations of the respective components of acceleration in x-, y- and z-directions are all related to the pressure gradients (modulo of viscous effects) and can be explained with the involved fluctuations of pressure (gradient) fields caused by vortices and high- and low-speed streaks. Especially, for the z-component of acceleration a remarkable four-leaves positive correlation area is visible with an average angle of ~+/- 32° wrt to the x- axis. Additionally, relatively strong negative correlation areas are present in-between these branches. Spanwise accelerations seem to be more coherently related to the orientation of involved vortices than the two other components. High values of spanwise accelerations can be found in streamwise oriented vortices, where all acceleration vectors point towards the pressure minimum of the vortex center line. A preferred orientation of +/- 32 ° of vortex axis in e.g. typical sweep streak events causing such (high) spanwise acceleration values is not described yet in the literature. The same pattern with opposite signs of correlation, but less prominent is visible for the x-component of acceleration (Figure 11, left), while the wall-normal acceleration component (Figure 11, middle) does not show such strong neighborhood dependencies, beside the typical streamwise elongation, which it shares with the x-component (see Figure 11, left). Further two-point correlations of the accelerations will be calculated at several wall distances and with various conditions in order to clarify the structural topologies involved in such statistical pattern formations of coherent structures.

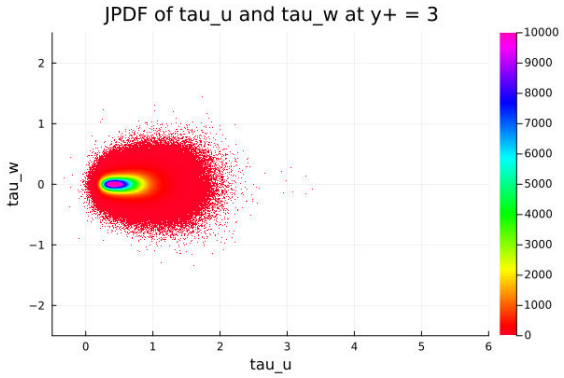

Figure 12 *Joint PDF of the wall shear stresses of $\tau_{w,x}$ and $\tau_{w,z}$ in a linear representation (color bar arbitrary values) and not normalized with the respective rms-values for derivatives calculated with velocity entries in a slice between 2.5 < y+ < 3.5*

In Figure 12 a joint PDF of $\tau_{w,x}$ and $\tau_{w,z}$ is shown in a linear representation, while the colors indicate an arbitrary number of entries per bin. One can see that the distribution calculated at this wall-distance is skew symmetric with a wide tail in positive direction and very few back-flow events on the negative side. For $\tau_{w,z}$ a zero mean and symmetric distribution for both sign-directions is given with a slightly wider distribution on the more positive side of $\tau_{w,x}$ than at that with smaller values. This indicates a higher probability of strong positive $\tau_{w,x}$ events in conjunction with larger $\tau_{w,z}$ events as on $\tau_{w,x}$ side with lower values as already shown in literature [14]. The corresponding width of the distributions or rms value for the streamwise component is almost twice the one for

the spanwise component of both τ_w. On the other hand, a more precise estimation of the involved uncertainty propagation for the calculation of the wall-shear stresses from different wall-normal distances needs to be performed based on the a-posteriori uncertainty quantification provided by the TrackFit [2] approach for both the particles position and velocity and the wall position in order to get normalizations with reliable rms-values corrected by the subtraction of the measurement noise contribution. The latter one might get quite significant very close to the wall. These steps for the qualification of 3D STB as a measurement tool for estimating mean and fluctuating wall-shear stresses have to be implemented in order to reach a data set for comparisons with DNS values of $\tau'_{w,x}$ and $\tau'_{w,z}$ and its rms from the literature.

6. Conclusions and outlook

A 3D STB measurement campaign has been carried out at four Reynolds numbers in the near wall region of ZPG -TBL flows in the 1-meter wind tunnel of DLR Göttingen. A new very accurate coordinate system- and wall vibration correction procedure has been proposed which allows to precisely position the wall with respect to the found tracks within ~ 400 nm accuracy. This is a mandatory step for all further processing steps and especially for a sound estimation of the instantaneous wall-shear stresses from the particle tracks. Profiles of mean velocity components and related Reynolds stresses have been calculated by bin averaging the particle tracks with a very high spatial resolutions in wall-normal direction (<1/5th wall unit step size). Two-point-correlations and (joint) PDFs of the various fluctuation components and wall-shear stresses have been calculated and partly shown and interpreted. These data are available for each bin with fully converged statistics even for higher-order moments. With this huge amount of time-resolved 3D velocity (gradient) field- and Lagrangian particle track data of near-wall TBL flows at four different moderate Reynolds numbers several investigations of flow structure dynamics and Lagrangian particle statistics have been and will be performed in future work:

We think about extensive investigations of the dynamics of rare reverse flow topologies and extreme positive wall-shear stress events in a spatial and temporal sense, determining high-resolution bin averaging profiles and related PDFs (down to ~1 µm per bin) for velocity and acceleration (up to third order moments), looking after instantaneous fields of both components of wall shear stress / friction velocity in relation to Q2- and Q4-events, checking the relation of time-resolved velocity gradients, acceleration and 3D pressure fields, tracking vortices, calculating 3D two-point space-time correlations of all available measures (velocity and acceleration components, velocity gradients, vorticity, pressure, wall-shear-stresses etc. pp.), estimating local energy dissipation rates, calculating torsion and curvature of tracks and look after the bending forces in the flow structures, determining two- particle dispersion relations over time in dependence of initial distance and y^+ position, calculating (co-)spectra from virtual sensors inside the time-resolved velocity fields and more.

References

[1] Schanz D, Gesemann S, Schröder A. (2016), Shake-The-Box: Lagrangian particle tracking at high particle image densities, Exp. Fluids, 2016, 57:570

[2] Gesemann S, Huhn F, Schanz D, Schröder A. (2016), From noisy particle tracks to velocity, acceleration and pressure fields using B-splines and penalties, Proceedings of 18th Intern Laser Symp, Lisbon, Portugal, 2016, July 4–7

[3] Godbersen P, Gesemann S, Schanz D, Schröder A. (2024), FlowFit3: Efficient data assimilation of LPT measurements, Int. Symp on Appl. Laser Techniques to Fluid Mechanics, Lisbon, Portugal, July 8 - 11, 2024

[4] Lenaers P, Li Q, Brethouwer G, Schlatter P and Örlü R. (2012), Rare backflow and extreme wall-normal velocity fluctuations in near-wall turbulence, Phys. Fluids, 2012, 24, 035110

[5] Chen X, Chung YM and Wan M. Backflow structures in turbulent pipe flows at low to moderate Reynolds numbers. J. Fluid Mech, 2023, vol. 966, A38

[6] Willert at al. (2018), Experimental evidence of near-wall reverse flow events in a zero-pressure gradient turbulent boundary layer, Experimental Thermal and Fluid Science, 2018, 91, 320

[7] Schröder A, Schanz D, Gesemann S, Willert C. (2015), Near-wall turbulence characterization using 4D-PTV Shake-The-Box, 11th Internl Symp on PIV- PIV2015, 14. - 16. Sept. 2015, Santa Barbara, CA, USA

[8] Willert C, Klinner J (2024): Dynamic Wall Shear Stress Measurement using Event-based 3D Particle Tracking, Int. Symp on Appl. Laser Techniques to Fluid Mechanics, Lisbon, Portugal, July 8 - 11, 2024

[9] Wieneke B (2008), Volume self-calibration for 3D particle image velocimetry, Exp Fluids 45:549–556

[10] Schanz D, Gesemann S, Schröder A, Wieneke B, Novara M (2013) Non-uniform optical transfer functions in particle imaging: calibration and application to tomographic reconstruction, Meas Sci Technol 24:024009
[11] Örlü R, Fransson JHM and Alfredsson PH (2010), On near wall measurements of wall bounded flows—the necessity of an accurate determination of the wall position, Prog Aero Sci 46:353–387
[12] Sclatter P and Örlü R (2010), Assessment of direct numerical simulation data of turbulent boundary layers. Journal of Fluid Mechanics. 2010; 659:116-126. doi:10.1017/S0022112010003113
[13] Örlü R and Schlatter P (2011), On the fluctuating wall-shear stress in zero pressure-gradient turbulent boundary layer flows, Phys.Fluids 23, 021704 (2011); doi: 10.1063/1.3555191
[14] Diaz-Daniel C, Laizet S and Vassilicos JC (2017), Wall shear stress fluctuations: Mixed scaling and their effects on velocity fluctuations in a turbulent boundary layer. Physics of Fluids 1 May 2017; 29 (5): 055102. https://doi.org/10.1063/1.4984002